

Quantum Turbulence: Achievements and Challenges

W.F. Vinen

Received: 12 June 2010 / Accepted: 20 September 2010 / Published online: 9 October 2010
© Springer Science+Business Media, LLC 2010

Abstract The paper is, for the most part, a review, written in its original form for an International Workshop on Vortices, Superfluid Dynamics, and Quantum Turbulence, held in Lammi, Finland, in 2010. Achievements are reviewed, and a strong emphasis is placed on problems that are either unsolved or still the subject of active discussion. These problems often call for more powerful experimental techniques, including local probes and actual visualization of the turbulent motion. Special emphasis is placed on recent progress in the development of visualization.

Keywords Superfluids · Quantum turbulence

1 Introduction

Quantum turbulence is the name we give to turbulence in a superfluid, in which the turbulent flow is influenced by quantum effects [1]. Turbulence has been studied extensively in the superfluid phase of liquid ^4He and in the superfluid B-phase of liquid ^3He , and it is starting to be studied in Bose-condensed gases. Except at the lowest temperatures these superfluids are two-fluid systems: a normal fluid coexisting with a superfluid component [2–6]. Flow of the superfluid component is, at low velocities, without dissipation, and rotational motion in a simply-connected volume can arise only through the presence of vortex lines [7], round each of which there is an irrotational circulation equal to $2\pi\hbar/m$, where m is the mass of a single atom in the case of a Bose system and the mass of two atoms in a Fermi system. In the presence of these quantized vortex lines there is a frictional interaction between the two fluids, known as *mutual friction* [8, 9].

W.F. Vinen (✉)
School of Physics and Astronomy, University of Birmingham, Birmingham B15 2TT, UK
e-mail: w.f.vinen@bham.ac.uk

In principle, turbulent flow is possible in either or both of these two fluids (although, as we shall see later, turbulence in the normal fluid of $^3\text{He-B}$ is inhibited by a large viscosity). Turbulence in the normal fluid is similar to that in a classical fluid, although its characteristics can be modified by mutual friction. Turbulence in the superfluid component must take the form of some more or less irregular tangle of quantized vortices [7], the motion of the vortices being modified by mutual friction.

The view is sometimes expressed that the most important and interesting case of quantum turbulence relates to that in the superfluid component at very low temperatures, where there is a negligible fraction of normal fluid (“pure” quantum turbulence). While it is true that this is a particularly interesting case, since it involves, for example, no viscous dissipation, types of turbulence involving both fluids are equally interesting and provide us with a rich variety of new types of turbulent phenomena, unknown in the study of classical turbulence.

A form of quantum turbulence (in a counterflow heat current in ^4He) was discovered almost sixty years ago [10–12]. In the Sects. 2 and 3 of this paper we aim to describe what has been discovered and understood since that time. The experimental tools available to us for the study of quantum turbulence have for much of this time been very limited. In Sect. 4 we shall review these tools and emphasize the need to develop more powerful experimental techniques. In the remaining sections we shall focus on a limited number of topics of special interest and draw attention to unsolved problems that present us with demanding challenges for the future.

2 Early History

2.1 Turbulence in a Thermal Counterflow

As soon as the two-fluid model of superfluid ^4He had been developed, it was realised that heat is carried in this liquid by a counterflow, the superfluid moving towards the source of heat, while the normal fluid moves away from it, with no net mass flow. At first sight the only dissipation that limits this process arises from the viscous flow of the normal fluid, but it was shown in 1949 [13] that, except at the smallest heat currents, there appeared also to be a dissipative force of mutual friction, acting between the two fluids. The origin of this force remained a mystery until experiments, especially those examining transient effects [10–12], showed that in all probability the mutual friction is associated with some form of turbulence in the superfluid component. Landau’s theory of superfluidity required that the flow of the superfluid component be irrotational [2, 3], so the idea arose that rotational motion of the superfluid was possible, but that it was accompanied, for some unknown reason, by mutual friction. It was this idea that led to the search for mutual friction in the uniformly rotating helium [8, 9]. In parallel with these experimental developments Feynman [7] suggested that it was quantized vortex lines that allowed the superfluid to rotate, and it was then immediately clear that the mutual friction, associated with either turbulence in the superfluid or uniform rotation, is caused by the frictional interaction between the normal fluid and the cores of the quantized vortices [9]. Interestingly, therefore, the first observation and study of quantum turbulence was intimately associated with the discovery of quantized vortices.

Experimental evidence [10–12] suggested that thermal counterflow turbulence in ^4He is essentially homogeneous, and that it might be generated and sustained by the action of the mutual friction on the quantized vortices in the superfluid component. Analysis of the results of these first experiments on thermal counterflow turbulence led to phenomenological equations describing the growth and decay of the turbulence and to suggested mechanisms of growth and decay [10–12]. But a serious understanding had to await the pioneering work of Schwarz [14]. Schwarz identified the essential physical processes underlying the way in which mutual friction in a counterflow can lead to a self-sustaining turbulent tangle of vortex lines. This essential physics can be seen by noting that mutual friction acting on a vortex ring in the appropriate direction can cause the ring to expand, and that this type of process can lead to a self-sustaining density of vortex rings, if, but only if, vortex reconnections [15] are allowed. It is interesting that mutual friction can in this way lead to the *generation* of turbulence, in spite of its being a dissipative process. Schwarz's work was based ultimately on his pioneering computer simulations, based on the vortex filament model in which the motion of a vortex is assumed to be governed by the principle that each element of a vortex moves with the local fluid superfluid velocity, as in classical fluid mechanics, but with two additional features: that vortices can reconnect if they approach each other closely, and that the vortex motion is modified through the Magnus effect when there is a force of mutual friction. His simulation of counterflow turbulence was based on the local induction approximation [1], which led to difficulties that he was able to overcome only with some *ad hoc* tricks. Very recently it has been shown by Adachi et al. [16] that these difficulties disappear if the local induction approximation is replaced by the more accurate Biot-Savart law, which takes proper account of long-range vortex-vortex interactions. We look forward to learning more about the results of these new simulations: for example, about the turbulent energy spectrum in the flow, and whether, for example, this spectrum indicates significant flow on scales larger than the vortex-line spacing (which is absent in the Schwarz simulations).

In spite of this impressive success in understanding thermal counterflow turbulence, there has remained a serious unsolved problem. The simulations that we have mentioned assumed that the flow of the normal fluid is laminar. Suggestions by Tough [17] that there is a critical heat current at which the character of the turbulence appears to change led Melotte and Barenghi [18] to suggest that this change might be a transition to turbulence in the normal fluid. We shall return later to some very recent evidence that this is indeed the case. An understanding of situations in which both fluids are turbulent in a counterflow provides us with a severe challenge.

2.2 Vortex Nucleation

There was an early recognition that any discussion of the way in which quantum turbulence can be generated must take account of the fact that the nucleation of quantized vortices is opposed by a serious potential barrier [19]. Near a solid boundary the barrier arises because a vortex is attracted to its image; in the bulk the generation of a small vortex ring, for example, lowers the energy of the system only if the ring exceeds a minimum size. At temperatures very close to the superfluid transition the barrier can be overcome thermally [19–22], but otherwise the barrier seems often to

be so large that it cannot be overcome at reasonable velocities (strictly speaking this is true only for the case of ^4He , with which all early experiments were concerned; the case of ^3He will be discussed later). It must then be the case that the growth of turbulence depends on the presence of existing remanent vortices, which might have been produced by the Kibble-Zurek mechanism [23] when the helium was first cooled through the transition temperature. Although fully-developed quantum turbulence may be unaffected by the details of the nucleation, it seems likely that critical velocities for the onset of the turbulence will be affected. This has been confirmed in recent beautiful observations by Hashimoto et al. [24]. These authors studied the critical velocity for a vibrating wire in a closed cell containing the ^4He , which could be filled slowly and at a low temperature through a very small channel. The idea is that such a filling procedure might well produce helium that is relatively free from remanent vortices. The authors did indeed observe a greatly increased critical velocity, which dropped as soon as a few vortices were deliberately introduced [25].

Generally speaking we have no means of knowing the configurations of remanent vortices, a fact that must always be borne in mind in interpreting experimental results.

2.3 Other Early Experiments

Quantum turbulence associated with a thermal counterflow has no classical analogue. During the early years a few experiments were reported in which quantum turbulence may have been produced in flows analogous to those in which turbulence can be produced in a classical fluid: examples are the torsional oscillations of a sphere in a fluid [26] and fluid oscillations in a U-tube [27]. Measurements were reported of the damping as a function of amplitude of oscillation, but interpretation proved difficult and unconvincing. Starting only in the mid-1990s were more powerful experimental techniques applied to the study of types of quantum turbulence that might have classical analogues. It is to these more recent studies that we now turn our attention.

3 Experimental Studies since 1995

There was a renaissance in the experimental study of quantum turbulence in about 1995, and we shall briefly describe the results.

3.1 Homogeneous Quantum Turbulence in Superfluid ^4He

Two experiments played an important role in this renaissance: that of Maurer and Tabeling [28]; and that of the Oregon group [29, 30].

Maurer and Tabeling generated turbulence in liquid helium by means of counter-rotating blades. They introduced a stagnation pressure probe into the helium at a point where there was a large steady flow velocity, U , on which the turbulent fluctuations, u were superimposed. The frequency spectrum of observed pressure fluctuations then reflected the spectrum of u^2 ; i.e. the turbulent energy spectrum. They observed the form of this spectrum at temperatures both above and below the superfluid transition (down to about 1.4 K). They observed no significant dependence on temperature. The

spectrum was of the form consistent with the classical Kolmogorov energy spectrum, $E(k)$, describing the way in which turbulent energy per unit mass is distributed over different length scales (inverse k) in homogenous isotropic turbulence in a classical inertial regime [31, 32]

$$E(k) = C\epsilon^{2/3}k^{5/3}, \quad (1)$$

where C is a constant of order unity and ϵ is the flux of energy towards shorter length scales in a classical Richardson cascade. In fact small deviations from Kolmogorov were also detected (associated with intermittency), and these too were unaffected by changes in temperature. These results showed rather clearly that quantum turbulence could be very similar to its classical counterpart, at least on scales larger than the size of the pressure transducer (of order 0.5 mm).

Classical homogeneous isotropic turbulence is often studied in the form of *grid turbulence*, formed by steady flow through a grid and observed at distances greater than a few mesh sizes behind the grid [32]. The Oregon group generated quantum turbulence in the wake of a steadily moving grid. They measured the vortex line density, L , as a function of distance behind the grid, by using a technique that had been developed in connection with the study of thermal counterflow turbulence: a measurement of the attenuation of second sound caused by the mutual friction arising from the presence of quantized vortex lines. In effect they measured the way in which the turbulence decayed in time. The interpretation of experiments of this type will be discussed critically later in this paper, but for the moment we can say that the results presented by the Oregon group are consistent with two assumptions: that on scales larger than the vortex line spacing (which we denote by $\ell = L^{-1/2}$ throughout this paper) the velocity fields of both fluids are essentially classical and are coupled together by mutual friction; and that dissipation occurs on smaller scales ($\leq \ell$) in accord with the formula

$$\epsilon = \nu' \kappa^2 L^2, \quad (2)$$

where κ is the quantum of circulation, and ν' is an effective kinematic viscosity.

We see that both experiments point to a flow of the superfluid component that is essentially classical on large scales, meaning scales large compared with the vortex spacing ℓ . We shall discuss the reason for this behaviour later. We emphasize at this stage that when there is coupled motion of the two fluids (as here, on scales much larger than ℓ), there is virtually no dissipation; movement of the two fluids with the same velocity ensures that there is no dissipation due to mutual friction, and it turns out that on scales much larger than ℓ viscous dissipation in the normal fluid can be neglected (for ^4He). Turbulence on scales much larger than ℓ is therefore in an inertial regime, which is necessary if the Kolmogorov spectrum is to hold.

3.2 Experiments with Vibrating Structures in ^4He

When a classical viscous fluid flows steadily past an obstacle at a small enough velocity the flow is laminar, but at higher velocities this laminar flow becomes unstable and gives way to what can be described loosely as turbulence (although the initial transition may be to a more regular form of rotational flow). It is of obvious interest

to enquire about the quantum analogues of this phenomenon, in which laminar viscous flow of the normal fluid and potential flow of the superfluid component gives way to quantum turbulence.

An experiment involving steady flow of superfluid helium past an obstacle is hard to achieve, especially if that flow must be free of vorticity (something similar to the pulled-grid arrangement of the Oregon group would be possible, but has not yet been attempted). However, it is relatively easy to set up an experiment in which the drag is measured on an obstacle oscillating in position in the helium. Many such studies have now been undertaken, and they have been reviewed in Skrbek and Vinen [33]; see also [48] for more recent work. The obstacle has been a small sphere [34–37], a cylinder in the form of a wire [24, 25, 38–42], a grid [43–46], or a small tuning fork [47, 48]. The experiments have covered a wide range of temperatures, down to those at which the fraction of normal fluid is negligible. The interpretation of the results is far from easy, the same being true of the classical analogues. We shall return to a brief discussion later.

3.3 The Decay of Quantum Turbulence in ^4He at Very Low Temperatures

Measurements of the decay of grid turbulence by the Oregon group were confined to temperatures above about 1.2 K, where there is a significant fraction of normal fluid. The dissipation, described by (2), is due to a combination of mutual friction and normal-fluid viscosity, which is fairly well understood [1]. It was appreciated by about 1995 that at very low temperatures this dissipative mechanism must disappear, with the consequence that either quantum turbulence does not then decay or some other dissipative processes become important. An early experiment by Davis et al. [49] showed that quantum turbulence in ^4He does decay even at very low temperatures, and an important paper by Svistunov [50], to which we shall refer later, discussed possible mechanisms. It is important to understand, of course, that a Kolmogorov spectrum requires the existence of a dissipative mechanism on some small length scale.

The first quantitative observations of the decay of quantum turbulence at a very low temperature were made in superfluid $^3\text{He-B}$, as we shall see in the next subsection. The first quantitative study of the decay of quantum turbulence at a very low temperature in ^4He was made in Manchester in 2007 [51]. The turbulence was generated by first setting a cell containing the helium into steady rotation, and then stopping the rotation (spin-down). Quantitative study required a method of measuring the line density as it decays in time, but the method used above 1 K, based on the attenuation of second sound, is no longer available because second sound ceases to propagate at low temperatures. The Manchester group developed a method based on the scattering by the vortex lines in the turbulent helium of small ($\sim 1 \mu\text{m}$) charged vortex rings that form when electron bubbles are injected into the helium. Evidence was produced that the spin-down generated turbulence that is approximately homogeneous and isotropic, and it was shown that the decay proceeded in a way that was similar to that observed in grid turbulence at higher temperatures, but at a somewhat slower rate. The Manchester group also observed the decay of turbulence generated by the injection of vortex rings. We shall present a critical discussion of these important results later.

3.4 Experiments with Superfluid $^3\text{He-B}$

From the point of view of quantum turbulence the vortices that can be formed in the B-phase of superfluid ^3He are expected to behave in a way that is fundamentally similar to those in ^4He , and during the past decade or so many interesting results with $^3\text{He-B}$ have been reported.

In spite of the fundamental similarities, there are, in the context of quantum turbulence, important detailed differences between ^4He and $^3\text{He-B}$.

- The normal fluid in ^3He has a very high viscosity, so that turbulence in the normal fluid is practically ruled out. The type of coupled turbulence that is seen in grid turbulence in ^4He is therefore impossible.
- The vortex core is much larger in $^3\text{He-B}$ than in ^4He , and even at very low temperatures it contains bound excitations that can contribute to dissipation.
- Vortex nucleation can be better controlled in $^3\text{He-B}$, owing to the larger vortex core size.
- By varying the temperature the magnitude of the mutual friction in $^3\text{He-B}$ can be varied over a wider range; in particular very large values can be achieved without approaching the critical temperature too closely.

Two groups have made substantial and important contributions to our knowledge and understanding of quantum turbulence in $^3\text{He-B}$.

Experiments by the *Helsinki group* [52, 53] have been concerned largely with the way in which the superfluid component is brought into rotation with a rotating vessel. (We shall not always give references to the original papers in cases where they can be found, as here, in convenient review articles.) A long tube containing the $^3\text{He-B}$ is set into rotation about its axis, which immediately leads to uniform rotation of the normal fluid, and it is arranged that one or more vortex lines are nucleated in the superfluid component at one end. NMR techniques are used to monitor the way in which the bulk of the superfluid is brought into rotation. At high temperatures, where the mutual friction is large, the nucleating vortex lines move smoothly along the tube, without multiplication, leading to uniform rotation to an extent determined by the number of lines. At lower temperatures, where the mutual friction is smaller, the motion of the vortex lines becomes chaotic, leading to the generation of quantum turbulence and, through reconnections, to the multiplication of lines. Eventually the whole of the superfluid is brought into rotation with the normal fluid. The process involves the propagation of a turbulent front along the tube, and much progress has been made in understanding the observed speed of propagation. Very recently, studies have been made of spin-up and spin-down occurring uniformly along the length of the tube, and it has been shown that the resulting flow in $^3\text{He-B}$ is much less likely to be turbulent than is the case with classical fluids or superfluid ^4He [54]. We shall comment on the results of some of these experiments later.

Experiments by the *Lancaster group* [55] have been concerned with the generation of quantum turbulence in $^3\text{He-B}$ by a vibrating wire or a vibrating grid at very low temperatures (no normal fluid), and they have developed a technique for some degree of visualization of the superfluid velocity field by Andreev scattering of thermal quasi-particles. Interpretation of the experiments with vibrating wires is complicated

by the fact that the critical velocity for the generation of quantum turbulence seems to be close to that for pair-breaking. Observations made with the vibrating grid are especially interesting. It seems that, as soon as a critical velocity of about 3 mm s^{-1} is exceeded, the vibrating grid produces a beam of small vortex rings. As the velocity of the grid increases the density of rings increases, until a coalesce of the rings produces fully-developed turbulence. The rate of decay of this fully developed turbulence, when the grid ceases to vibrate, can then be measured. Interesting observations have also been made of the fluctuations and spatial correlations in the line density [56], similar to those reported by Roche et al. for ^4He [57]. We shall return to these results later.

3.5 Experiments with Bose-Condensed Gases

Very recently interesting experiments on turbulent motion in very cold, Bose-condensed, gases have been reported [58]. As we shall see more clearly in the next section, studies of quantum turbulence in ^4He and $^3\text{He-B}$ have suffered because it is difficult to find methods by which the flows can be visualized; in particular it has been difficult to visualize the vortex lines. In the case of Bose-condensed gases visualization of the vortex lines is relatively easy, although it is generally destructive.

It is too early to assess what might be achieved by studying quantum turbulence in Bose-condensed gases. It is worth remarking that a Bose condensed gas is notably different from superfluid ^4He in a number of important respects. The ratio of the size of the core of a vortex to typical vortex separations is very much larger; indeed in a Bose-condensed gas this ratio is typically of order unity (instead of $\sim 10^{-5}$ as in ^4He). This has a major effect on dissipation in quantum turbulence. As we shall explain in a later section, dissipation in ^4He at very low temperatures (no normal fluid) is associated with the formation of a Kelvin-wave cascade, which carries energy to motion on a very small length scale, where it can be dissipated by phonon radiation; some phonon emission is associated with reconnections (also involving small length scales) but the small size of the vortex core ensures that this loss of energy is relatively small. This situation is very different in a Bose-condensed gas, where most of the dissipation is associated with phonon emission during reconnections, and where therefore any Kelvin-wave cascade is likely to be unimportant. Another important difference lies in the fact that Bose-condensed gases are confined to small volumes, in which the fluid density is not constant; any study of large scale turbulence, especially homogeneous turbulence, is therefore ruled out. Bose-condensed gases do have an important advantage over ^4He , in that they are described rather accurately by the Gross-Pitaevskii equation; this means, for example, that we have a good microscopic theory for a vortex reconnection in a Bose-condensed gas [15], which does not exist for a reconnection in ^4He . A serious experimental study of vortex reconnections in a Bose-condensed gas would be very useful. An experimental study of the production of a turbulent wake behind an obstacle would seem to be feasible in a Bose-condensed gas, and the possibility of actually seeing what is happening in this case, where remanent vortices are not playing any role, would be interesting and important.

4 Experimental Techniques

We have mentioned a number of experimental techniques in our historical introduction. Here we aim to summarize the techniques that are, or soon will be, available to us, and we assess their power.

As in the study of classical fluids, we can measure forces that are exerted on solid boundaries by the flowing helium. These forces can be in the form of pressure or temperature gradients along channels, or they can be forces on solid objects in the flow. These forces give us little or no direct information about the detailed form of the flow.

Various techniques are available for the measurement of vortex-line densities. In the case of ^4He above 1 K a measurement of the attenuation of second sound gives the mutual friction per unit volume, which is directly related to the vortex density [8, 10–12]. Local vortex-line densities can be measured if the second sound propagates in a limited volume [57], but the spatial resolution is inevitably rather poor. In the case of ^4He below 1 K, where second sound does not propagate, line densities can be measured from the scattering of small vortex rings, as already explained. Again spatial resolution is poor. In the case of $^3\text{He-B}$ an NMR signal is modified by flow of the superfluid component [52], and this can form the basis of a measurement of vortex density. In the case of $^3\text{He-B}$ at a very low temperature, Andreev scattering of thermal quasi-particles is related to superfluid velocity fields; this rather subtle technique has been developed and exploited by the Lancaster group [55], who have used it to determine vortex densities with some spatial resolution. The character of an Andreev scattered beam may contain within it information about details of turbulent structures, as is being investigated at present by Barenghi and Sergeev (private communication). The best spatial resolutions attainable with these techniques are probably of order 1 mm, which is generally much larger than much of the structure in a typical quantum turbulent flow.

Study of classical turbulence is often facilitated by the use of local probes, which are sensitive to local velocities. The hot-wire anemometer does not work in a superfluid, and laser-Doppler techniques require seeding, to which we refer below. A pressure probe, such as that used by Maurer and Tabeling [28], can measure pressure fluctuations, which, observed in the appropriate circumstances, are related to the turbulent energy spectrum; the spatial resolution is limited by the size of the sensor, which is typically about 1 mm for commercially available sensors. Attempts are being made to develop sensors with better spatial resolution, but such resolution, combined with the necessary sensitivity, will be hard to achieve (Ihas, private communication).

The suggestion has been made that a small structure, such as a wire or a tuning fork, vibrating at a small amplitude, might be sensitive to a local turbulent intensity. Preliminary experiments suggest that any effects might be very hard to interpret.

Especially at the lowest temperatures the heat capacity of a superfluid is very small, so the rate of decay of turbulent energy can be measured as a rate of rise in temperature (this was first mentioned by Samuels and Barenghi, in the context of a random vortex tangle [59]). We shall refer to this type of measurement as *calorimetric*. In principle, as we shall see later, a measurement of the rate of decay of turbulent energy would be a very useful complement to a measurement of the rate of decay of

line density. Attempts to develop this technique in connection with the decay of grid turbulence in ^4He are in progress [60], and some observations of a temperature rise accompanying the decay of turbulence in $^3\text{He-B}$ are reported at this Workshop.

Although these various techniques have been used in clever ways to obtain much information about quantum turbulence, attempts to visualize the flow in ways that are so important in the study of classical turbulence have for many years proved unsuccessful. During the past five years this situation has changed. Two problems have impeded progress: finding and introducing into the helium suitable tracer particles, which must be small enough to track small scale motions, be roughly neutrally buoyant in a fluid of low density, and be visible; and the interpretation of the results, when there are three possibly relevant velocity fields, those of the normal and superfluid components and of the quantized vortices [61].

A number of different types of tracer particle have been used: hollow glass spheres (diameter $\sim 100\ \mu\text{m}$); polymer microspheres ($\sim 1\ \mu\text{m}$); particles of solid hydrogen or solid hydrogen/deuterium mixtures ($\sim 1\ \mu\text{m}$); and metastable He_2 triplet-state excimer molecules. Except in the case of the excimer molecules special techniques have had to be developed to introduce an appropriate density of the particles into the helium, avoiding coagulation. All the work reported so far has been with ^4He above 1 K.

Van Sciver and his colleagues [61], using for the most part micron-sized polymer microsphere as tracers, have studied thermal counterflow, with Particle Image Velocimetry. Intriguing results have been reported, but they are proving hard to interpret, and it is becoming evident that PIV may be ill-suited to a situation where there is more than one velocity field.

Lathrop and his group [62–64] have used micron-sized (or more recently sub-micron-sized) particles of solid hydrogen, combined with particle tracking techniques. Again they have studied thermal counterflow. They have discovered that some of their particles follow the normal fluid, while others are trapped on, and follow the motion of, the quantized vortices. They have provided strikingly direct evidence of the counterflow associated with a heat current. They have discovered that sometimes a particle trapped on a vortex undergoes a motion caused by a vortex reconnection (the first direct evidence for reconnections), and they have made a detailed study of this motion.

The loading of the tracer particles used by both the Van Sciver and the Lathrop groups into the helium involves fairly elaborate techniques, and it would therefore be difficult to apply their methods at temperature below 1 K. McKinsey and his group [65–68] are developing the use of metastable triplet-state He_2 excimer molecules as tracers. Such molecules can be generated in helium easily by electron irradiation, and they form bubble states with a diameter of about 0.5 nm. Particles of this size can be expected to follow the normal fluid at temperatures above 1 K, and to be trapped on vortex lines below 1 K. They can be detected and imaged by laser fluorescence. We shall describe this technique in more detail later, where we shall also report briefly on the application of the technique to the study of normal-fluid motion in a thermal counterflow.

The development of these techniques for the visualization of quantum turbulence promises to transform the subject. Not only will we be able, for the first time, to see what is really going on, but visualization can facilitate the acquisition of much

more detailed information about quantum turbulence than has hitherto been possible. An example of such detailed information is provided by turbulent structure functions, as explained later.

5 Homogeneous Isotropic Quantum Turbulence at Very Low Temperatures

We shall now discuss in more detail measurements that have been reported on the especially interesting case of homogeneous quantum turbulence at very low temperatures, where, as we have already emphasized, there is little or no normal fluid to provide mechanisms for dissipation. These measurements are interesting in themselves, and they throw up many challenging problems.

Practically all relevant existing measurements relate to the decay of vortex-line density, and, as we have explained, they have come for ^4He from the Manchester spin-down experiments [51], and for $^3\text{He-B}$ from the Lancaster vibrating grid experiments [55]. Interesting experiments have also been reported that relate to turbulence generated by the coalescence of small vortex rings in ^4He [69]. It is likely that this same generating mechanism operates in the Lancaster vibrating grid experiments. Experiments to study grid turbulence in ^4He at low temperatures are in progress but have yet to produce meaningful results [60]. Experiments at low temperatures on the rate of propagation of a turbulent front in $^3\text{He-B}$, to which we have already referred [52], also provide information about dissipation, although in relation to turbulent flows that are not homogeneous; the results are discussed in other contributions to this Workshop.

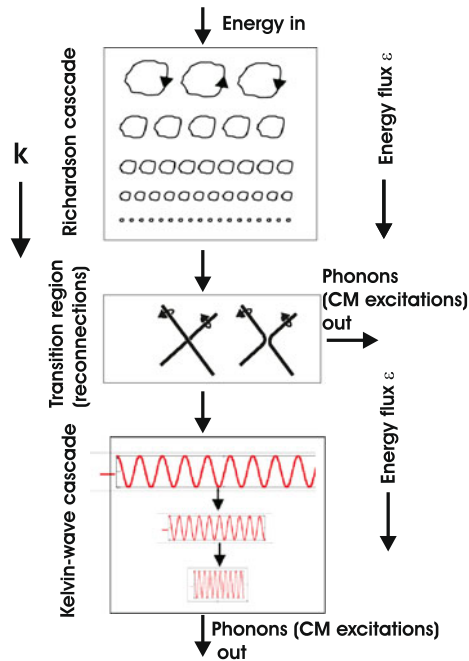
5.1 Introductory Theory

In order to facilitate the discussion we shall first outline important aspects of the theory that is believed to describe the essential phenomena that are involved in the decay of quantum turbulence at very low temperatures.

Suppose first that the turbulence exists in a steady state, in which energy is fed in at a rate ϵ per unit mass on a scale, R , which is large compared with the vortex spacing, ℓ ; dissipation at the rate ϵ occurs on a small scale ($< \ell$). Our present theoretical understanding is summarized in Fig. 1, in which the length scale is decreasing (wave vector, k , increasing) as we move down the diagram.

On scales large compared with ℓ the turbulence is essentially classical (we call it *quasi-classical*). Owing to non-linear turbulent interactions, there is a Richardson cascade [31] that leads to a flux of energy, equal to ϵ , to smaller and smaller length scales; there is no dissipation on these scales (an inertial range), so ϵ is constant, independent of k . The large-scale motion in the superfluid is achieved by partial polarization of the vortex lines. As in classical turbulence there is a Kolmogorov energy spectrum, given by (1). On scales comparable with or less than ℓ the motion cannot be classical, and we can ask why this has little effect at large scales, in view of the fact that non-linear interactions couple motion on different length scales. The widely accepted reason is that the non-linear interactions are local in k -space; in other words motion on one length scale is strongly coupled only to motion on adjacent length

Fig. 1 (Colour online)
Illustrating the probable pattern
of decay of quantum turbulence
at very low temperatures



scales. This means that the Richardson cascade is indeed a cascade: energy flows from one length scale to the next adjacent length scale, and then to the next adjacent length scale, and so on. It follows that the behaviour on a large ($\gg \ell$) scale is unaffected by processes occurring on a scale of order or less than ℓ , and therefore unaffected by quantum effects. The same assumption of locality in k -space underlies the Kolmogorov spectrum, which is unaffected by the mechanism of dissipation. Computer simulations of quantum turbulence by Tsubota and his colleagues [70, 71], using both the vortex filament model and the Ginsburg-Pitaevskii equation, have produced energy spectra that are at least consistent with a Kolmogorov spectrum on scales greater than ℓ .

On scales small compared with ℓ one obvious type of motion that we can envisage is a Kelvin wave on a vortex line. It is widely believed that such wave motion can carry energy to smaller and smaller scales, through non-linear interactions between waves of different wave numbers. In other words the energy flux is associated with a form of wave turbulence [72–74]. Whether there is a simple Kelvin-wave cascade, arising from wave interactions that are local in k -space, will be discussed at this Workshop. A process envisaged by Feynman in which energy flows to small scales by the break-up of small vortex rings was shown by Svistunov [50] to violate conservation of energy and impulse.

At zero temperature, and in ^4He , energy is ultimately dissipated by radiation of sound (phonons) by the Kelvin waves, but this process can occur only at very high wave numbers, of order 10^9 m^{-1} [76–78]. At finite temperatures there can be dissipation of the Kelvin waves by a small residual mutual friction. In $^3\text{He-B}$ energy can probably be absorbed by the bound excitations in the vortex core (the Caroli-Matignon

excitations [79]), when the Kelvin-wave frequency matches the spacing between energy levels of these excitations.

Finally there must be a transition region, at scales of order ℓ (but possibly extending over a couple of decades in length scale), separating the quasi-classical regime from the Kelvin-wave cascade. The structure of the turbulence within this transition has been the subject of much discussion [80–84]. In principle there could be a bottleneck at this transition [80], arising from a difficulty in matching the fluxes of energy in the quasi-classical and Kelvin wave regimes. There is little doubt that vortex reconnections play an important role in the generation of the Kelvin-wave cascade, but the details, including the possible existence of a bottleneck, remain controversial. It is known that reconnections are dissipative [75], in the sense that they involve some emission of phonons. However, in superfluid helium, in which the ratio of vortex core size to vortex spacing is typically very small, this dissipation is relatively unimportant [1].

It is important to understand that the turbulent regime that we have been describing is in a steady state, so that the energy flux ϵ is constant in time. In all the experiments that have so far been carried out at low temperatures, the turbulence is decaying; there is no continuous input of energy and no steady state. In favourable circumstances this is not important. For example, suppose that we have only a quasi-classical Richardson cascade, and that the size of the largest eddies is limited by the dimensions of a containing vessel. Most of the energy is in the largest (“energy-containing”) eddies, which decay at a rate, determined by their turnover time (see later), which is larger than the characteristic times associated with the smaller eddies. Thus, as the turbulence decays, the energy-containing eddies act as a energy reservoir that gradually feeds energy into the cascade at a rate ϵ , while at any given time the smaller eddies are in a quasi-steady state corresponding to the instantaneous energy flux ϵ . However, this simplifying situation does not always apply, as we shall see later.

It is interesting to ask what would happen if energy were injected on a length scale within the transition region. There might then be some flux of energy towards larger length scales, but perhaps the rate of dissipation of energy, occurring, as we suggest, only at a very high wave number, is unchanged. We might then be looking at the decay of a random tangle of lines, without any large-scale motion. Experimental evidence will be discussed in the next section. Any flux of energy towards larger length scales may be unimportant, for the following reason. As in the case discussed by Stalp et al. [30], this flux is likely to lead to a spectrum on scales larger than the line spacing that is proportional to k^2 , and we assume, tentatively, that this spectrum joins smoothly to the spectrum ($\sim k^{-1}$) on scales smaller than the line spacing; in that case it is easy to show that the turbulent energy on scales larger than the line spacing is much smaller than that on smaller scales.

5.2 Experimental Evidence

All the experimental evidence relates to the rate of decay of vortex line density, and it is summarised in Figs. 2–4. Figure 2 relates to ^4He in which the turbulence is generated by spin-down [51]. Figure 3 relates to ^4He in which the turbulence is generated by a short (0.1–0.3 s) burst of charged vortex rings [69]. We see that during a final

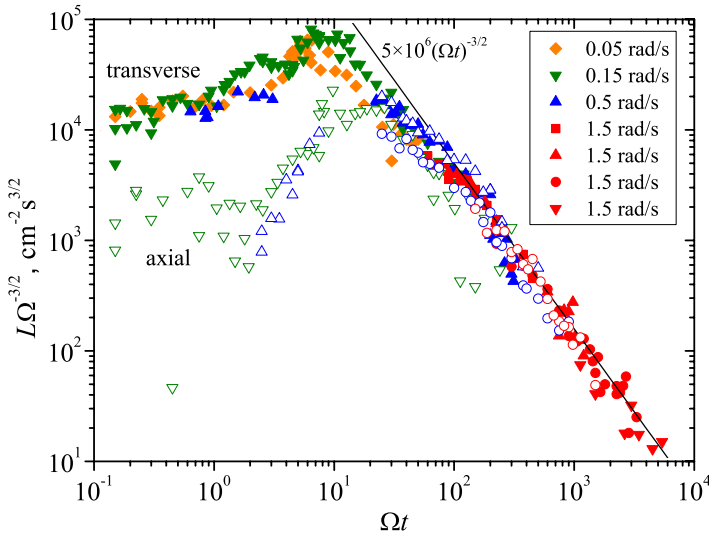


Fig. 2 (Colour online) Decay of line density, L , with time, t , in the Manchester spin-down experiment: $L\Omega^{3/2}$ plotted against Ωt , for different initial angular velocities of rotation, Ω ; “axial” and “transverse” refer to the directions in which the probing vortex rings are injected [51]

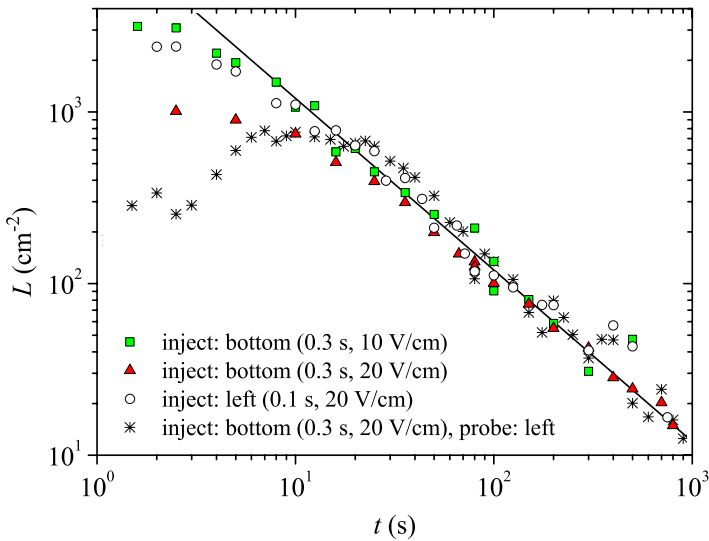


Fig. 3 (Colour online) Decay of line density, L , with time, t , in the Manchester experiment in which the turbulence is generated by a short burst of vortex rings [69]

decay (large times) the line density produced by spin-down falls as $t^{-3/2}$, while that produced by short bursts of charged vortex rings falls as t^{-1} . Very recently, Walmsley and Golov (private communication) have studied the decay of turbulence generated by bursts of charged vortex rings of variable length; they find that for lengths greater

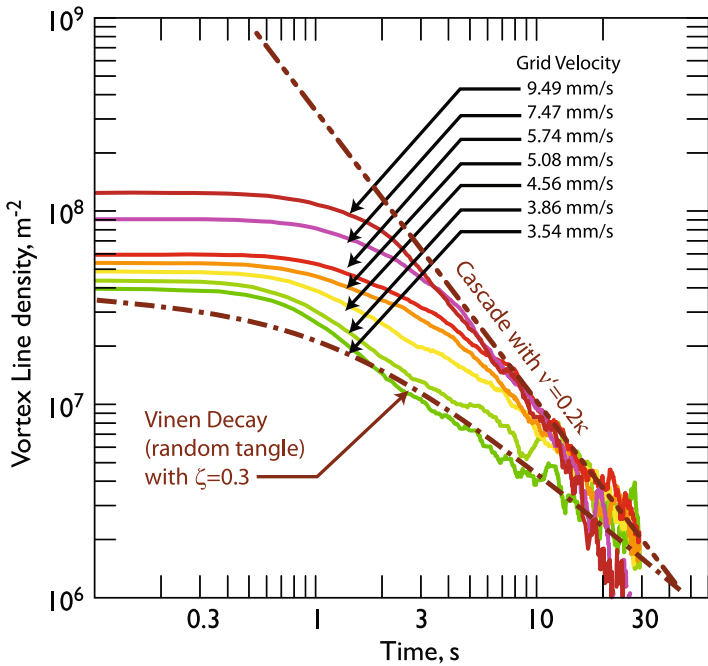


Fig. 4 (Colour online) Decay of line density with time in ³He-B in the Lancaster experiment. The time, *t*, is measured from the time at which the grid motion is turned off. The different curves relate to different initial grid velocities, as shown. The parameter ζ is related to v' by the relation $\zeta = 4\pi v' / (\Delta\kappa)$

than roughly 100 s the final decay has a form ($t^{-3/2}$) similar to that observed in the spin-down experiments, and that for intermediate lengths, in the range of roughly 5–20 s, the final decay starts as t^{-1} but then changes to $t^{-3/2}$. Figure 4 relates to ³He-B in which the turbulence is generated by, probably, the coalescence of uncharged vortex rings produced by a vibrating grid. Here we see that at large initial line densities the final decay has the form $t^{-3/2}$, while at smaller initial line densities it has the form t^{-1} [85].

We shall not attempt to analyse these decay curves in all their details. Instead we shall focus on only the behaviour at large times. As we have just seen, this behaviour is rather simple. The line density decays with time as t^{-n} , where *n* is either 3/2 or unity. In some cases there is a period during which there is decay with $n = 1$, after which the value of *n* seems to switch to $n = 3/2$.

A decay at large times as $t^{-3/2}$ was seen first by Stalp et al. [30] in ⁴He at temperatures above 1 K, and these authors suggested how such a time dependence could arise in quasi-classical turbulence. A decay as t^{-1} was implicit in the phenomenological treatment of decaying turbulence in a thermal counterflow. In the next section we shall outline the arguments that lead to these two time-dependences, using the minimum number of assumptions.

5.3 Assumptions that Lead to the Decay of Vortex Density as Either $t^{-3/2}$ or t^{-1}

First, we make the following assumptions.

- The decay follows the pattern illustrated in Fig. 1.
- Most of the turbulent energy is concentrated in the largest (quasi-classical) eddies. This is the case for classical homogeneous turbulence, for which the Richardson cascade is cut off by viscosity at a wave number equal to $\epsilon^{1/4} \nu^{-3/4}$.
- The lifetime of the largest eddies is equal to their turnover time, D/U , where D is the size of these eddies and U is the characteristic velocity in these eddies. If the assumption is made that the lifetimes of *all* eddies are equal to their turnover times, then the Kolmogorov spectrum follows.
- The size D remains constant as the decay proceeds.
- The dissipation per unit mass is given by

$$\epsilon = \nu' \kappa^2 L^2, \quad (3)$$

where ν' is an effective kinematic viscosity. This is based on the assumption that the dissipation is determined entirely by the length scale ℓ .

It is then easily shown that in the limit of large times the following relations hold

$$E_C = 2D^2 t^{-2}, \quad \epsilon = 4D^2 t^{-3}, \quad L = \frac{2D}{\kappa \nu'^{1/2}} t^{-3/2}, \quad (4)$$

where we have denoted the turbulent energy by E_C , in order to emphasize that it is concentrated in the quasi-classical eddies.

Now we make the following assumptions.

- There is no quasi-classical motion; i.e. no motion on scales greater than ℓ .
- The turbulent energy per unit mass is that associated with a random tangle of vortices, spacing ℓ , and is therefore given by

$$E_Q = \frac{\kappa^2}{4\pi} L \Lambda, \quad \Lambda \sim \ln \frac{\ell}{\xi}, \quad (5)$$

where ξ is the vortex core parameter, and where we have denoted the turbulent energy by E_Q to emphasize that this is a “quantum energy” in the sense that it arises from motion on scales of order or less than the vortex line spacing.

- Dissipation is still given by (3).

It is then easily shown that in the limit of large times

$$L = \frac{\Lambda}{4\pi \nu'} t^{-1}. \quad (6)$$

We see then that our two sets of assumptions have produced line densities that vary with time as $t^{-3/2}$ and t^{-1} , in accord with the two observed types of behaviour. We note that the dependence on time as t^{-1} is observed only when the turbulence is generated by the injection of small vortex rings (radius less than ℓ), so that our

identification of this time dependence with turbulence existing only on scales of order or less than ℓ is not unreasonable. But we note also that the injection of charged vortex rings for longer periods can lead to a time dependence as $t^{-3/2}$, and that in the case of ^3He the time-dependence seems to depend on the initial line density.

The constancy of D , which is required to obtain the $t^{-3/2}$ behaviour, is assumed to arise because the size of the largest eddies is limited by the size of the cell in which the turbulence is generated.

5.4 Values of the Effective Kinematic Viscosity

Let us assume now that our analyses have correctly described the two different observed time-dependences, and let us use the experimental data to obtain values of the effective kinematic viscosity, ν' . The results are summarized in Fig. 5, where we have plotted the dimensionless kinematic viscosity, ν'/κ , against the dimensionless mutual friction parameter α [1], which decreases towards zero with decreasing temperature. The value of D is taken to be the size of the cell or width of the channel containing the ^4He , or, in the case of ^3He , the measured size of the decaying turbulent cloud (obtained by using the Andreev reflection technique). Values of ν' for the higher temperatures (above 1 K) relate to the grid turbulence that was studied by Stalp et al. [86]. Especially at low temperatures, there seems to be a rather confused picture, with different experiments yielding very different values of ν'/κ . Values relating to a time-dependence as t^{-1} are of order, or a little greater than, 0.1, while those relating to a time dependence as $t^{-3/2}$ range from 3×10^{-3} to 0.3. Values for ^3He are consistently larger than those for ^4He .

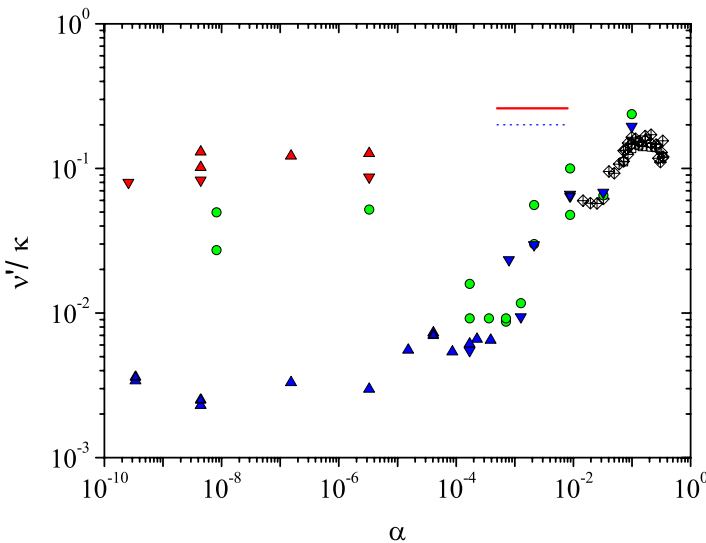


Fig. 5 (Colour online) Values of the effective kinematic viscosity plotted against temperature, for different types of experiment. Upper triangles (red): ^4He , short pulse of injected charged rings (t^{-1}); circles (green): ^4He , long pulses of injected charged rings ($t^{-3/2}$); lower triangles (blue): ^4He , spin down; squares and diamonds: ^4He above 1 K from Stalp et al. [30]; upper line (red): ^3He , small grid velocity (t^{-1}); broken line (blue): ^3He , large grid velocity ($t^{-3/2}$)

5.5 Comments, Questions and Problems

The results that we have just presented raise many questions, which we can summarise as follows.

- Why are the values of the effective kinematic viscosity for ^3He so different from those for ^4He ? It is true that dissipation may take place by different processes within the Kelvin-wave cascade, and that the quantum of circulation has a slightly different value, but it is not clear how these differences can lead to very different values of the effective kinematic viscosity. The turbulence observed in the experiments on ^3He is not confined by the walls of a container, and therefore cannot be strictly homogeneous, and this fact may be relevant. A critical discussion of the interpretation of the experimental results for ^3He , particularly as they relate to decays as $t^{-3/2}$, has been given by Golov and Walmsley [87].
- Our derivation of the time-dependence as $t^{-3/2}$ does not require that the whole spectrum at large scales ($\gg \ell$) has the Kolmogorov form, so experimental evidence for this spectrum is weak.
- Our derivation of (4) was based on the assumption that $E_C \gg E_Q$. It is easily proved, from the various equations that we have already written down, that

$$\frac{E_Q}{E_C} = \frac{\Lambda}{2\pi} \left(\frac{\kappa}{v'} \right)^{2/3} \left(\frac{\ell}{D} \right)^{2/3}. \quad (7)$$

It turns out that this ratio is not small in the case of the Manchester spin-down experiments at the lowest temperature. Typically it is equal to about 3.6 even at the start of the period when the decay goes as $t^{-3/2}$, although at higher temperatures, towards 1 K, there is no problem. Thus our derivation of the $t^{-3/2}$ law is invalid at the lowest temperature, yet this law still appears to be obeyed.

- Do we understand, in the case of ^4He , why a short pulse of injected charged vortex rings leads to decay as t^{-1} , whereas a long pulse leads to decay as $t^{-3/2}$? We need large-scale eddies for the $t^{-3/2}$ decay law. Perhaps the total impulse associated with a long pulse of rings is quite large, so that not only are the rings created but also there is a net backflow on a scale of order the size of the containing cell; and perhaps the electric field applied to a high density of charged vortex rings can create a large-scale flow. Another possible puzzle is that the random tangle produced by a short pulse of injected rings is observed to diffuse more rapidly throughout the volume of the Manchester cell [69] than might be expected [88, 89]. A more detailed understanding of these issues would be helpful.
- A important possibility is that there is uncertainty in the size and lifetime of the largest eddies. As we have mentioned, the dimension D in the Manchester experiments is taken to be the side of the cubical cell in which the helium is contained, and the lifetime is assumed to be D/U . There is a strong hint that the effective value of either D or the time D/U may not be the same for spin-down turbulence as it is for turbulence created by a pulse of charged rings. Perhaps the assumed values of D and D/U are wrong in the situation where, as we have seen, the inequality $E_C \gg E_Q$ seems to be violated. Perhaps, for example, the lifetime is much larger than D/U at the lowest temperatures, because it is enhanced by a conservation

of angular momentum following the spin-down, this effect being more serious at lower temperatures owing to the absence of normal fluid. Some evidence against this suggestion comes from a recent observation in Manchester that the decay is not modified by the addition of shallow grooves in the inside walls of the containing vessel, which might be expected to modify the boundary conditions. Nevertheless, we must conclude that the true values of ν' at low temperatures remain seriously uncertain.

- There is some evidence that in ^4He the value of ν' is strongly reduced when energy is fed to small scales through a quasi-classical Richardson cascade. This suggests that polarization of the vortex tangle reduces ν' . Again, however, ^3He seems to behave differently.
- Nemirovskii [89] has suggested that the turbulent decay could be enhanced by diffusion of vortex lines to the boundary of the cell, a view that is based on his calculations that the diffusion takes place more rapidly than was observed in the simulations of Tsubota et al. [88]. The fact that the data displayed in Fig. 2 lie on a single curve for large times, independently of the angular velocity from which spin-down takes place, is evidence against this view, but some residual uncertainty remains.
- It has been argued, especially by Kozik and Svistunov [84], that the way in which ν' varies with temperature in the Manchester spin-down experiments can be used as evidence for the validity of detailed theories of the structure of the transition region and of the way in which it feeds energy into the Kelvin-wave cascade. The serious uncertainty that we now see in the values of ν' must cast doubt on these arguments. The comment might also be added that there is in reality virtually no experimental evidence for the existence of a Kelvin-wave cascade.
- We recall that our derivations of the time-dependence of the decay of line density were based on the assumed validity of (3). Theories of the structure of the transition region support this assumption, but they are based on an assumed steady state in which the line density is independent of time, so that the energy flux, ϵ , is constant throughout the inertial cascades. In practice there is not a steady state and the flux will be different at different points in the cascades. This means that (3) cannot apply at all points in the cascades. This is clearly an important matter that requires further investigation.

We conclude that many experimental facts relating to the decay of homogeneous isotropic quantum turbulence at very low temperatures are still not reliably established, and that there are serious uncertainties relating to the application of the analyses set out in Sect. 5.3.

5.6 New Experiments

We turn now to a brief discussion of possible new experiments that may help to resolve some of these uncertainties.

All the experimental measurements at very low temperatures that we have discussed so far relate to the decay of vortex line density. As we have already noted, it ought to be possible to measure also the decay of total turbulent energy. Looking,

for example, at (4), we see that such a calorimetric measurement could provide information about the effective value of D , in contrast to a measurement of the decay in vortex density, which yields only the ratio $D/(\nu')^{1/2}$. Since, as we have emphasized, the effective value of D is open to question, such a calorimetric measurement could be very valuable. More detailed analysis shows that such a measurement could also tell us something about the total energy associated with length scales of order or less than ℓ , which could then be compared with the predictions of theories relating to the turbulent structure in the transition and Kelvin-wave regions.

We have noted that experiments so far tell us virtually nothing about the existence and characteristics of a Kelvin-wave cascade. One suggestion here is that we should attempt to carry out an experiment similar to that described by Hall [90] when he first showed that Kelvin waves can propagate on an array of quantized vortices. His apparatus consisted of a horizontal circular disc, suspended from a torsion fibre in uniformly rotating ^4He above 1 K; the dynamical behaviour of the disc indicated clearly that Kelvin waves were generated on the vortices that were attached to the roughened disc. Above 1 K the Kelvin waves were damped by mutual friction, but well below 1 K this damping disappears and a Kelvin-wave cascade should be generated on each vortex. The observed damping on the disc would tell us the rate at which energy is being fed into the cascades, and a calorimetric measurement would tell us the rate at which energy is being dissipated by phonon radiation. In a steady state these two quantities must be equal, but otherwise their difference measures the rate of increase in turbulent energy stored in the cascade. A major challenge would be to ensure that imperfect pinning of the vortices on the surface of the disc does not lead to dissipation.

Ideally, of course, we would like to have local probes for use at very low temperatures. Andreev scattering of thermal quasi-particles can provide information with some spatial resolution in ^3He , and it might be possible to develop small pressure sensors. However, such pressure sensors would require what may be prohibitively high sensitivity, because the maximum turbulent velocities that can be generated in quantum turbulence at very low temperatures are seriously limited by the requirement that the decaying turbulence does not produce too much heating. The ideal local probe would be a tracer particle attached to a vortex. In the long run, metastable excimer molecules might fulfil this role.

6 Visualization of Superflow with Metastable He_2 Excimer Molecules

We have emphasized the importance, as we see it, of recent developments in the visualization of quantum turbulent flow. The use of micron-sized hydrogen particles in conjunction with particle tracking techniques to visualize flow in superfluid ^4He is reviewed by Lathrop at this Workshop. Here we shall review recent progress with the use of metastable He_2 excimer molecules [68]. These excimer molecules can be produced by electron bombardment of the helium or, probably, by laser excitation. Molecules are produced both in singlet states, which decay very rapidly, and in triplet states, which are metastable and have a lifetime in liquid helium of about 13 s. The metastable molecules exist as bubble states, with a bubble radius of about 0.53 nm.

Fig. 6 (Colour online) Energy level diagram for the triplet-state He₂ molecule

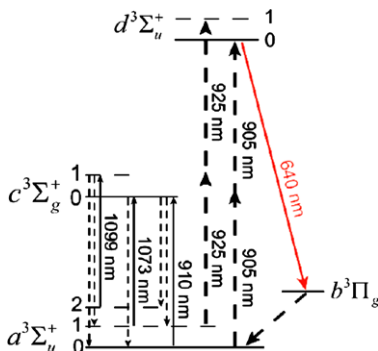
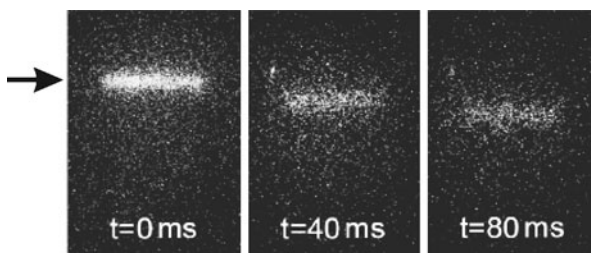


Fig. 7 Photographs of a line of excimer molecules at different times after tagging. The arrow shows the initial position of the tagged molecules. Temperature: 1.95 K; heat flux: 640 mW cm⁻² [68]



The energy-level diagram for the metastable molecule is shown in Fig. 6. The molecules are illuminated with a laser at 905 nm, when they are excited by two-photon absorption to the $d^3\Sigma_u^+$ state. They fluoresce at 640 nm, and return to the ground state, from which they can again be excited and fluoresce (we omit some of the details). This cyclic process allows a given molecule emit a succession of fluorescent photons, at a wavelength very different from that of the exciting laser. Filtering at 640 nm will then allow the imaging of the molecules, without interference from the exciting laser. A particular group of molecules can be “tagged” in a way that is described by Rellergert et al. [66] (essentially the molecules are raised to an excited vibrational state), so that they fluoresce when excited at 925 nm instead of 905 nm, although each of these tagged molecules emits only one fluorescent photon and cannot be cycled.

Most recently this technique has been applied to a preliminary study of the flow of the normal fluid in a thermal counterflow in ⁴He [68]. At the relevant temperatures (above 1 K) the molecules are expected to follow the motion of the normal fluid, so that it ought to be possible to determine whether or not this motion is turbulent. The heat flow takes place along a vertical glass tube of square (5 mm × 5 mm) cross-section. At the closed top end of the tube there is a chamber containing the heater and a source of metastable excimer molecules. Under the influence of the heat current the molecules move downwards along the tube, being carried by the normal fluid and eventually filling the tube. With an appropriate well-focussed laser beam (the pump) a thin horizontal line of molecules in the tube is tagged, and the motion of these molecules is tracked as a function of time with a probe laser, as shown in Fig. 7.

We see that the tagged molecules move downwards along the glass tube, and the average velocity with which they move proves to agree with the average expected

normal-fluid velocity. We see also that the initially thin line of molecules spreads out. The spreading is much larger than would be expected from ordinary diffusion. It is therefore attributed to turbulence in the normal fluid, so providing evidence that the normal fluid is indeed turbulent in this particular experiment.

It should be explained that the photographs in Fig. 7 are superpositions of some 40 separate exposures, each exposure relating to a given time interval after tagging. The photographs represent therefore averages over 40 different realizations of the turbulent velocity field. The need to average in this way arises from the fact that the tagged molecules cannot be cycled, so that averaging is required in order to achieve an acceptable signal. If a line of molecules could be created, through laser-field ionization, by a well-focussed femtosecond laser pulse, and then examined by cyclic fluorescence, such averaging would not be required. The line would then be seen to distort with time, the distortion being related to the transverse structure functions for the turbulence [31]. The relative motion of two parallel lines would be related to the longitudinal structure functions. This improvement in the technique could make it much more powerful. As it is, the broadening of the line is related in part to the time-dependence of the separation of two particles in a turbulent flow (see, for example, [91]), but it is influenced also by the way in which the line of molecules is distorted by the turbulent motion on a scale larger than the width of the molecular line; these two effects are difficult to disentangle.

We see from Fig. 7 that the average velocity profile of the normal fluid appears to be flat. This is probably due to a combination of the turbulence and the non-linear average mutual friction in the heat current. It should be noted that the technique we have described can be applied only at fairly large heat currents, because otherwise the excimer molecules are not pulled into the region of observation before they decay. Therefore it has not yet been possible to use the technique to observe a critical velocity below which the normal fluid is not turbulent; the existence of such a critical velocity has been predicted by Melotte and Barenghi [18]. Indirect evidence for such a critical velocity has come from an experiment in which the motion of a small bunch of molecules is tracked as it moves along the centre line of the tube; we refer to the paper for details [68].

This new technique, especially in a version that does not require tagging, promises to have many applications; for example, in obtaining rather direct information about the energy spectrum in quantum grid turbulence.

7 The Generation of Quantum Turbulence by Vibrating Structures

We have already remarked that the classical analogue of this case is generally very complicated. While the same is not necessarily true of the quantum case, there is at least the possibility that the quantum case is also complicated and therefore hard to understand in any detail. This is especially the case if, as now, we have no available visualizations of the flow, and if, at a finite temperature, we must allow for flow of both the normal and superfluid components. We can of course be guided by computer simulations, and in some cases such simulations have indeed provided us with valuable insight [25, 92]. But realistic computer simulations are difficult to set up, for

several reasons: it is difficult to allow for the inevitable roughness of the surface of the vibrating structure; the simulations are as yet not capable of dealing adequately with coupled motion of the two fluids; and a full understanding of the transition to fully-developed turbulence often requires a simulation that incorporates a larger number of vortices than can be treated with existing computer programmes.

In the quantum case authors have often focussed almost exclusively on the identification of a critical velocity at which there is rapid growth in the density of vortex lines. This is analogous to the identification of the velocity in a classical system at which the first instability occurs in the laminar flow. However, this is not the whole story, since the way in which the flow evolves at higher velocities is also interesting and important, as we see very clearly in the classical cases [33]. In the quantum case the only available data at supercritical velocities take the form usually of plots of the drag against velocity, or, better, of plots that use the relevant dimensionless parameters. Unfortunately, it is sometimes difficult in the quantum case to reach velocities at which the limiting high-velocity behaviour is clearly evident.

One difficulty that arises in thinking about critical velocities is the possibility that these velocities depend on a particular configuration of remanent vortices. That this can certainly be the case is evident in the recent work on Hashimoto et al. [24], in which the critical velocity is greatly increased by careful preparation of the helium. However, it may be the case that, as long as there is some minimum density of remanent vortices, there is a rapid growth in vortex density (an avalanche) at a critical velocity that is independent of this minimum density. This idea underlies the theory of Hänninen and Schoepe [93]. This theory is based on the idea that an avalanche can be described by a generalization by Kopnin of an equation that was originally written down in connection with thermal counterflow, and it describes the rate of change in line density when the superfluid moves at a uniform, time-independent, velocity relative to a fixed normal fluid. There are some difficulties with this argument. The Kopnin derivation is based on the HVBK equations, which are subject to a course-grained averaging. The course-grained vorticity is then put equal to κL , which cannot be strictly true since the line density is related to the enstrophy rather than the vorticity. The generalization to an oscillating flow is also questionable. Nevertheless, the idea that there is an avalanche may indeed be true, and there are signs that it is true in the simulations of Hänninen et al. [92]. Hänninen and Schoepe show that according to their model the critical velocity should be of order $(\kappa\omega)^{1/2}$, where ω is the angular frequency of oscillation, independently of the shape and size of the oscillating structure. There is some evidence that such a relation does hold, but is not totally persuasive, as discussed by Blázquez et al. [48]. There is a shortage of studies in which any dependence of critical velocity on the shape and size of a structure has been systematically investigated, and the range of frequencies that have been investigated is generally rather small. In any case a critical velocity that is of order $(\kappa\omega)^{1/2}$ can arise in other ways. For example, suppose that a remanent vortex is pinned to the surface of the structure. Oscillation of the structure at frequency ω will generate Kelvin waves on the vortex with half-wavelength $\sim(\kappa/\omega)^{1/2}$. Vortex self-reconnection at the surface of the structure will then produce loops with radius $R \sim (\kappa/\omega)^{1/2}$, and these loops will expand only if the velocity amplitude exceeds $\kappa/R \sim (\kappa\omega)^{1/2}$. More complicated theories, such as that of Skrbek and Vinen [33],

which are based on quasi-classical processes, also give similar critical velocities. It is not obvious how at this stage we can say which theory is most nearly correct. And there remains the question of our understanding the form of the drag *versus* velocity curve at supercritical velocities.

Interesting switching effects are often observed just above the critical velocity [36]. These have been analysed in considerable detail, but they do not seem to throw much light on the fundamental mechanisms of the breakdown of laminar (or potential) flow. A number of worrying features have emerged in recent experimental results, especially at very low temperatures and with both vibrating grids and vibrating tuning forks: a lack of reproducibility between results obtained with what appear to be very similar structures; a time-dependent excess damping at velocities that are less than that normally identified as the critical value; and other strange time-dependent phenomena that are reminiscent of level-crossing effects, due possibly to acoustic coupling (private communications from the Lancaster groups). All in all, we seem still to be very far from understanding the behaviour of oscillating structures in a superfluid. Although some elegant and instructive experiments have been carried out with oscillating structures (for example those of Hashimoto et al. [24] and Goto et al. [25]), there is a growing feeling among some of us that the study of many oscillating structures at the present time is not adding significantly to our understanding of quantum turbulence. This situation could change if visualization techniques were to become available for use with these structures.

8 Comments and Conclusions

It is clear that quantum turbulence is becoming a rich field of study. Many different forms of turbulent behaviour have been identified, many of which are not seen in classical turbulence and are therefore new to physics. Although we have been able to identify many of these forms of quantum turbulence, we must ask whether our supposed understanding of them is based on secure experimental foundations. In this connection there is an urgent need for more powerful experimental techniques, especially with local probes, and more especially still with actual visualization. Recent progress with the development of useful forms of visualization has been very promising.

Acknowledgements Many physicists and applied mathematicians have contributed to our present knowledge and understanding of Quantum Turbulence. I am extremely grateful to very many members of this community, too many to list, for stimulating discussions. Inevitably, this review has had to be selective, and my personal interests have perhaps played too large a role in my choice of material. I have been unable to discuss adequately, or even mention, many important studies of quantum turbulence. To the authors of these studies I apologize. I am grateful to Wei Guo, Andrei Golov and Shaun Fisher for supplying me with a number of the figures used in this review.

References

1. W.F. Vinen, J.J. Niemela, *J. Low Temp. Phys.* **128**, 167 (2002)

2. L.D. Landau, J. Phys. Mosc. **5**, 71 (1941)
3. L.D. Landau, J. Phys. Mosc. **11**, 91 (1947)
4. L. Tisza, Nature **141**, 913 (1938)
5. L. Tisza, J. Phys. Radium **1**, 165 (1940)
6. L. Tisza, J. Phys. Radium **1**, 350 (1940)
7. R.P. Feynman, in *Progress in Low Temperature Physics*, vol. 1, ed. by C.J. Gorter (North Holland, Amsterdam, 1955), Chap. 2
8. H.E. Hall, W.F. Vinen, Proc. R. Soc. A **238**, 204 (1956)
9. H.E. Hall, W.F. Vinen, Proc. R. Soc. A **238**, 215 (1956)
10. W.F. Vinen, Proc. R. Soc. A **240**, 114 (1957)
11. W.F. Vinen, Proc. R. Soc. A **240**, 128 (1957)
12. W.F. Vinen, Proc. R. Soc. A **242**, 493 (1957)
13. C.J. Gorter, J.H. Mellink, Physica **15**, 285 (1949)
14. K.W. Schwarz, Phys. Rev. B **38**, 2398 (1988) and references therein
15. J. Koplik, H. Levine, Phys. Rev. Lett. **71**, 1375 (1993)
16. H. Adachi, S. Fujiyama, M. Tsubota, Phys. Rev. B **81**, 104511 (2010)
17. J.T. Tough, in *Progress in Low Temperature Physics*, vol. VIII, ed. by D.F. Brewer (North-Holland, Amsterdam, 1982), p. 133
18. D.J. Melotte, C.F. Barenghi, Phys. Rev. Lett. **80**, 4181 (1998)
19. W.F. Vinen, in *Liquid Helium: Proc. Int. School of Physics Enrico Fermi, Course XXI* (Academic Press, New York, 1963), p. 336
20. S.V. Iordanskii, Sov. Phys. JETP **21**, 467 (1965)
21. J.S. Langer, M.E. Fisher, Phys. Rev. Lett. **19**, 560 (1967)
22. J.S. Langer, J.D. Reppy, in *Progress in Low Temperature Physics*, vol. 6, ed. by C.J. Gorter (North Holland, Amsterdam, 1970), p. 1
23. W.H. Zurek, Nature **317**, 505 (1985)
24. N. Hashimoto, R. Goto, H. Yano, K. Obara, O. Ishikawa, T. Hata, Phys. Rev. B **76**, 020504 (2007)
25. R. Goto, S. Fujiyama, H. Yano, Y. Nago, N. Hashimoto, K. Obara, O. Ishikawa, M. Tsubota, T. Hata, Phys. Rev. Lett. **100**, 045301 (2008)
26. C.B. Benson, A.C.H. Hallett, Can. J. Phys. **34**, 668 (1956)
27. R.J. Donnelly, O. Penrose, Phys. Rev. **103**, 1137 (1956)
28. J. Maurer, P. Tabeling, Europhys. Lett. **43**, 29 (1998)
29. M.R. Smith, R.J. Donnelly, N. Goldenfeld, W.F. Vinen, Phys. Rev. Lett. **71**, 2583 (1993)
30. S.R. Stalp, L. Skrbek, R.J. Donnelly, Phys. Rev. Lett. **82**, 4831 (1999)
31. U. Frisch, *Turbulence* (Cambridge University Press, Cambridge, 1995)
32. G.K. Batchelor, *The Theory of Homogeneous Turbulence* (Cambridge University Press, Cambridge, 1953)
33. L. Skrbek, W.F. Vinen, in *Progress in Low Temperature Physics*, vol. XVI, ed. by M. Tsubota, W.P. Halperin (Elsevier, Amsterdam, 2009) and references therein. Chap. 4
34. J. Jäger, B. Schuderer, W. Schoepe, Phys. Rev. Lett. **74**, 566 (1995)
35. M. Niemetz, H. Kerscher, W. Schoepe, J. Low Temp. Phys. **126**, 287 (2002)
36. M. Niemetz, W. Schoepe, J. Low Temp. Phys. **135**, 447 (2004)
37. W. Schoepe, Phys. Rev. Lett. **92**, 095301 (2004)
38. H. Yano, A. Handa, H. Nakagawa, M. Nakagawa, K. Obara, O. Ishikawa, T. Hata, J. Phys. Chem. Solids **66**, 1501 (2005)
39. H. Yano, A. Handa, H. Nakagawa, K. Obara, O. Ishikawa, T. Hata, M. Nakagawa, J. Low Temp. Phys. **138**, 561 (2005)
40. H. Yano, A. Handa, M. Nakagawa, K. Obara, O. Ishikawa, T. Hata, in *American Institute of Physics Conference Proceedings*, vol. 850 (American Institute of Physics, Melville, 2006), p. 195
41. H. Yano, N. Hashimoto, A. Handa, M. Nakagawa, K. Obara, O. Ishikawa, T. Hata, Phys. Rev. B **75**, 012502 (2007)
42. D.I. Bradley, D.O. Clubb, S.N. Fisher, A.M. Guéault, R.P. Haley, C.J. Matthews, G.R. Pickett, K. Zaki, J. Low Temp. Phys. **138**, 493 (2005)
43. H.A. Nichol, L. Skrbek, P.C. Hendry, P.V.E. McClintock, Phys. Rev. Lett. **92**, 244501 (2004)
44. H.A. Nichol, L. Skrbek, P.C. Hendry, P.V.E. McClintock, Phys. Rev. E **70**, 056307 (2004)
45. W.F. Vinen, L. Skrbek, H.A. Nichol, J. Low Temp. Phys. **135**, 423 (2004)
46. D. Charalambous, P.C. Hendry, P.V.E. McClintock, L. Skrbek, W.F. Vinen, Phys. Rev. E **74**, 036307 (2006)

47. M. Blázquez, D. Schmoranzler, L. Skrbek, Phys. Rev. E **75**, 025302 (2007)
48. M. Blázquez, D. Schmoranzler, L. Skrbek, W.F. Vinen, Phys. Rev. B **79**, 054522 (2009)
49. S.I. Davis, P.C. Hendry, P.V.E. McClintock, Phys. B, Condens. Matter **280**, 43 (2000)
50. B.V. Svistunov, Phys. Rev. B **52**, 3647 (1995)
51. P.M. Walmsley, A.I. Golov, H.E. Hall, A.A. Levchenko, W.F. Vinen, Phys. Rev. Lett. **99**, 265302 (2007)
52. V.B. Eltsov, R. de Graaf, R. Hänninen, M. Krusius, R.E. Solntsev, V.S. L'vov, A.I. Golov, P.M. Walmsley, in *Progress in Low Temperature Physics*, vol. XVI, ed. by M. Tsubota, W.P. Halperin (Elsevier, Amsterdam, 2009), and references therein. Chap. 2
53. A.P. Finne, V.B. Eltsov, R. Hänninen, N.B. Kopnin, J. Kopu, M. Krusius, M. Tsubota, G.E. Vovolik, Rep. Prog. Phys. **69**, 3157 (2006)
54. V.B. Eltsov, R. de Graaf, P.J. Heikkinen, J.J. Hosio, R. Hänninen, M. Krusius, V.S. L'vov, Phys. Rev. Lett. **105**, 125301 (2010)
55. S.N. Fisher, G.R. Pickett, in *Progress in Low Temperature Physics*, vol. XVI, ed. by M. Tsubota, W.P. Halperin (Elsevier, Amsterdam, 2009) and references therein. Chap. 3
56. D.I. Bradley, S.N. Fisher, A.M. Guénault, R.P. Haley, S. O'Sullivan, G.R. Pickett, V. Tsepelin, Phys. Rev. Lett. **101**, 065302 (2008)
57. P.-E. Roche, P. Diribarne, T. Didelot, O. Français, L. Rousseau, H. Willaime, EPL **77**, 66002 (2007)
58. E.A.L. Henn, J.A. Seman, G. Roati, K.M.F. Magalhães, V.S. Bagnato, J. Low Temp. Phys. **158**, 435 (2010)
59. D.C. Samuels, C.F. Barenghi, Phys. Rev. Lett. **81**, 4381 (1998)
60. G.G. Ihas, G. Labbe, S.C. Lui, K.J. Thompson, J. Low Temp. Phys. **150**, 384 (2008)
61. S.W. Van Sciver, C.F. Barenghi, in *Progress in Low Temperature Physics*, vol. XVI, ed. by M. Tsubota, W.P. Halperin (Elsevier, Amsterdam, 2009), and references therein. Chap. 5
62. G.P. Bewley, D.P. Lathrop, K.R. Sreenivasan, Nature **441**, 588 (2006)
63. M.S. Paoletti, R.B. Fiorito, K.R. Sreenivasan, D.P. Lathrop, J. Phys. Soc. Jpn. **77**, 111007 (2008)
64. M.S. Paoletti, M.E. Fisher, K.R. Sreenivasan, D.P. Lathrop, Phys. Rev. Lett. **101**, 154501 (2008)
65. D.N. McKinsey, W.H. Lippincott, J.A. Nikkel, W.G. Rellergert, Phys. Rev. Lett. **95**, 111101 (2005)
66. W.G. Rellergert, S.B. Cahn, A. Garvan, J.C. Hanson, W.H. Lippincott, J.A. Nikkel, D.N. McKinsey, Phys. Rev. Lett. **100**, 025301 (2008)
67. W. Guo, J.D. Wright, S.B. Cahn, J.A. Nikkel, D.N. McKinsey, Phys. Rev. Lett. **102**, 235301 (2009)
68. W. Guo, S.B. Cahn, J.A. Nikkel, W.F. Vinen, D.N. McKinsey, Phys. Rev. Lett. **105**, 045301 (2010)
69. P.M. Walmsley, A.I. Golov, Phys. Rev. Lett. **100**, 245301 (2008)
70. T. Araki, M. Tsubota, S.K. Nemirovskii, Phys. Rev. Lett. **89**, 145301 (2002)
71. M. Kobayashi, M. Tsubota, Phys. Rev. Lett. **94**, 065302 (2005)
72. W.F. Vinen, M. Tsubota, A. Mitani, Phys. Rev. Lett. **91**, 135301 (2003)
73. E. Kozik, B. Svistunov, Phys. Rev. Lett. **92**, 035301 (2004)
74. E. Kozik, B. Svistunov, Phys. Rev. Lett. **94**, 025301 (2005)
75. M. Leadbeater, T. Winiecki, D.C. Samuels, C.F. Barenghi, C.S. Adams, Phys. Rev. Lett. **86**, 1410 (2001)
76. W.F. Vinen, Phys. Rev. B **61**, 1410 (2000)
77. W.F. Vinen, Phys. Rev. B **64**, 134520 (2001)
78. E. Kozik, B. Svistunov, Phys. Rev. B **72**, 172505 (2005)
79. C. Caroli, J. Matricon, Phys. Kondens. Mater. **3**, 380 (1965)
80. V.S. L'vov, S. Nazarenko, O. Rudenko, Phys. Rev. B **76**, 024520 (2007)
81. V.S. L'vov, S. Nazarenko, O. Rudenko, J. Low Temp. Phys. **153**, 140 (2008)
82. J. Laurie, V.S. L'vov, S. Nazarenko, O. Rudenko, Phys. Rev. B **81**, 104526 (2010)
83. E. Kozik, S.V. Svistunov, Phys. Rev. B **77**, 060502 (2008)
84. E. Kozik, S.V. Svistunov, Phys. Rev. Lett. **100**, 195302 (2008)
85. D.I. Bradley, D.O. Clubb, S.N. Fisher, A.M. Guénault, R.P. Haley, C.J. Matthews, G.R. Pickett, V. Tsepelin, K. Zaki, Phys. Rev. Lett. **96**, 035301 (2006)
86. S.R. Stalp, J.J. Niemela, W.F. Vinen, R.J. Donnelly, Phys. Fluids **14**, 1377 (2002)
87. A.I. Golov, P.M. Walmsley, J. Low Temp. Phys. **156**, 51 (2009)
88. M. Tsubota, T. Araki, W.F. Vinen, Physica B **329**, 224 (2003)
89. S.K. Nemirovskii, Phys. Rev. B **81**, 064512 (2010)
90. H.E. Hall, Proc. R. Soc. A **245**, 456 (1958)
91. P.A. Davidson, *Turbulence* (Oxford University Press, London, 2004)
92. R. Hänninen, M. Tsubota, W.F. Vinen, Phys. Rev. B **75**, 064502 (2007)
93. R. Hänninen, W. Schoepe, J. Low Temp. Phys. **153**, 189 (2008)